Journal of Computational Acoustics, Vol. 9, No. 1 (2001) 101–123

PRECISION CORRELATIONS BETWEEN THE GEOACOUSTIC PARAMETERS OF AN UNCONSOLIDATED, SANDY MARINE SEDIMENT

MICHAEL J. BUCKINGHAM

Marine Physical Laboratory, Scripps Institution of Oceanography, University of California, San Diego 9500 Gilman Drive, La Jolla, CA 92093-0238, USA

Institute of Sound and Vibration Research, The University, Southampton SO17 1BJ, England

Received 1 January 2000
Revised 1 June 2000

A recently introduced theoretical model of wave propagation in an unconsolidated, sandy marine sediment is discussed in this article. Essentially, the model consists of four analytical expressions, which specify four wave properties of the sediment, namely the speed and attenuation of the compressional and the shear wave. These expressions contain just three unknown constants, which must be evaluated from data. A technique is described in which these constants are determined from measured values of the compressional wave speed, the shear wave speed, and the shear wave attenuation. This technique is applied to preliminary data from O.N.R.s SAX'99 recent experiment on a sandy sediment in the Gulf of Mexico. From the fully specified equations, the fourth wave property, the attenuation of the compressional wave, is computed and found to lie within 0.5 dB/m of the measured value. Based on this limited evidence, it appears that the wave properties of an unconsolidated sediment are highly correlated and predictable. According to the theory, the causal connections between the wave properties originate in the sliding of one micro-asperity against another on the surfaces of contact between contiguous grains in the medium.

1. Introduction

An unconsolidated, sandy marine sediment supports a compressional wave with phase speed, c_p, in the region of 1700 m/s (somewhat faster than that of the pore water), and a much slower shear wave with phase speed, c_s, of about 100 m/s. The actual values of c_p and c_s depend on the grain size and the porosity, and both wave speeds show logarithmic dispersion. In unconsolidated granular materials, experimental investigations[1–5] have failed to reveal the presence of a compressional wave of the second kind, the so-called slow wave of the Biot theory,[6,7] although the slow wave has been detected[8] in a consolidated granular medium in which the grains were fused together to form an elastic skeletal frame. The fact that the slow wave in an unconsolidated sediment is negligible or absent indicates that the flow of pore fluid through the interstices between grains is in-significant as far as wave propagation is concerned. This implies that the wave properties are independent of the permeability of the unconsolidated medium, a conclusion that is supported by experimental evidence from Wyllie *et al.*,[9] who found that the speed of the compressional wave through water-

saturated glass beads remained constant as the permeability was varied by over four orders of magnitude.

Considerable experimental evidence indicates that the attenuation of the compressional wave[10−12] and of the shear wave[13,14] in an unconsolidated sandy sediment both scale essentially as the first power of frequency, f, or equivalently that the quality factor, Q, is, in both cases, independent of frequency. For a medium sand (grain diameter $\approx$ 400 micrometers) the attenuation coefficient of the shear wave is $\alpha_s \approx 30$ dB/m/kHz, whereas the attenuation of the compressional wave is substantially lower at $\alpha_p \approx 0.3$ dB/m/kHz. As with the wave speeds, the actual values taken by the attenuations depend on the grain size and the porosity. The Biot theory,[6,7] in which the primary dissipation mechanism is interstitial flow of the viscous pore fluid, does not yield a constant Q but instead predicts attenuations that scale as f^2 at low frequencies, evolving into $f^{1/2}$ beyond some threshold frequency.

The subject of the present article is the inter-relationships between the wave properties, namely the compressional and shear wave speeds and attenuations, and the physical properties of an unconsolidated sandy marine sediment. Such correlations are known to exist, and have been represented empirically by Hamilton and Bachman[15] and Richardson,[16] who used regression analyses to fit polynomials or exponentials to extensive experimental data sets. This differs from the approach described below, in which the expressions developed between the various geoacoustic parameters characterizing the sediment are derived from a theoretical model[17,18] of wave propagation in an unconsolidated granular medium. An underlying tenet of the model is that the unconsolidated granular material possesses no skeletal elastic frame. The central physical mechanism in the model is shearing at grain-to-grain contacts,[19] which introduces rigidity and dissipation into the material. The rigidity, *inter alia*, supports the propagation of a shear wave, and the dissipation leads to compressional and shear wave attenuations with constant Q, both in accord with experimental observations.

The grain-shearing theory leads to analytical expressions for the four wave properties, that is, the speed and attenuation of the compressional and the shear wave. By making certain approximations, these expressions reduce to simple algebraic forms. From these approximate expressions, several sets of values, representing realistic marine sediments, were generated recently, and these values were incorporated into some of the benchmark models of range-dependent environments used in the O.N.R.-sponsored, SWAM'99 workshop that was held at the Naval Postgraduate School, Monterey, CA in September 1999. More details of the workshop can be found in other papers in this special issue of the Journal of Computational Acoustics.

Unlike the empirical representations of correlations between the geoacoustic parameters of an unconsolidated granular medium, the grain-shearing theory leads naturally to such correlations because it rests on a single causative mechanism, namely the sliding of one micro-asperity against another on the surfaces of contact between contiguous grains. In the present article, the exact expressions for the wave properties that emerge from the theory are examined carefully. It is shown that the four expressions involve only three unknown constants, which may be evaluated by comparison with three, single-frequency data points for a specific sediment: the shear wave speed, the shear wave attenuation, and the

compressional wave speed. The fourth wave property, the compressional wave attenuation for the same sediment, is then predicted from the theory and shown to be almost identical to the measured value. To begin, the significant physical properties of the sediment are discussed as a prelude to considering the wave properties and the predicted correlations, which constitute the main theme of the paper.

2. Physical Properties

The physical properties of an unconsolidated sediment that are relevant to wave propagation in the medium are the mean grain diameter, u_g, the porosity, N, the bulk density, ρ_o, and the bulk modulus, κ. These quantities are not independent of one another. The bulk density is related to the porosity through the weighted mean

$$\rho_o = N\rho_w + (1-N)\rho_g\,, \tag{2.1}$$

where $\rho_g = 2650$ kg/m^3 is the density of the mineral grains (quartz) and $\rho_w = 1024$ kg/m^3 is the density of the pore fluid (seawater). Similarly, the bulk modulus of the sediment is given by the weighted mean

$$\frac{1}{\kappa} = N\frac{1}{\kappa_w} + (1-N)\frac{1}{\kappa_g}\,, \tag{2.2}$$

where $\kappa_g = 3.36 \times 10^{10}$ Pa is the bulk modulus of the mineral grains (quartz) and $\kappa_w = 2.25 \times 10^9$ Pa is the bulk modulus of the pore fluid (seawater).

An interesting feature of the porosity of an unconsolidated sediment is that it depends on the grain size. This is illustrated in Fig. 1(a), where the measured porosity (symbols), taken from Hamilton[10,20] and Richardson and Briggs,[21] shows a decreasing trend with increasing grain diameter. Such behavior is in distinct contrast with the close-packing arrangements, either regular or random, of smooth, uniform-size spheres; all such packing structures exhibit a porosity that is independent of the sphere size. Of course, sand grains, in general, are not smooth spheres but possess some degree of roughness. An important physical effect of the surface roughness is to allow pore fluid to percolate between grains, thus raising the porosity above the value that would obtain for a similar packing of smooth spheres.

The grain roughness may also be responsible for the variation of the porosity with grain size shown in Fig. 1(a). Based on this idea, a simple model[17] of a sandy sediment with a uni-modal grain-size distribution has been introduced in which the assumption that the grains are smooth has been relaxed. By treating the grains as randomly packed, slightly roughened spheres of uniform (mean) size, the following relationship between the porosity and the grain diameter is obtained from a straightforward packing analysis:

$$N = 1 - P\left\{\frac{u_g + 2D}{u_g + 4D}\right\}^3\,, \tag{2.3}$$

where $P = 0.63$ is the packing factor of a random arrangement of smooth spherical grains and D is the r.m.s. height of the surface roughness on each of the grains. Equation (2.3)

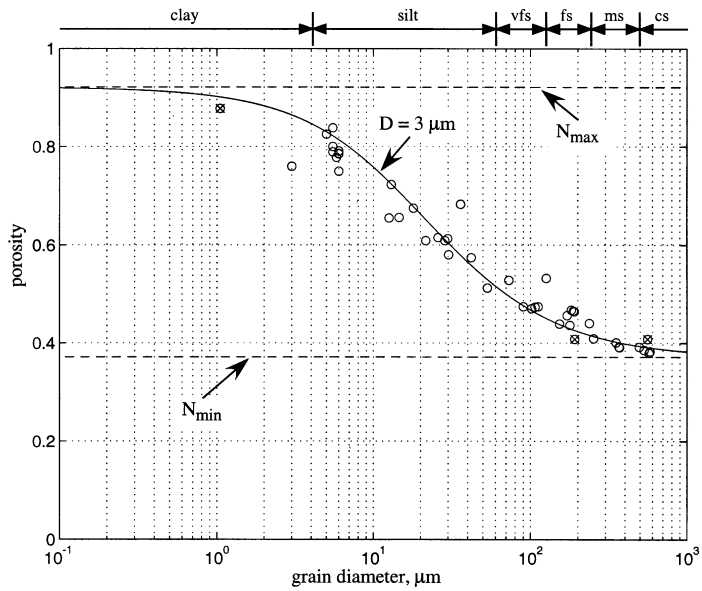

(a)

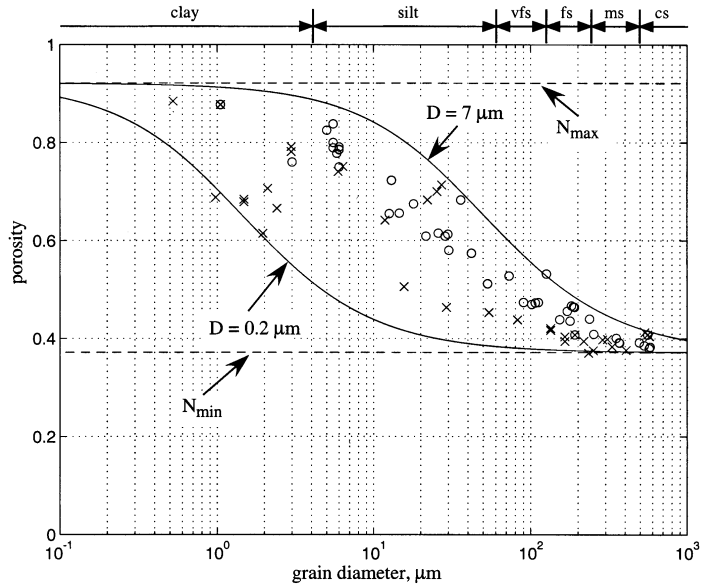

(b)

Fig. 1. Porosity versus grain size for unconsolidated marine sediments. The symbols represent data from Hamilton[10,20] (circles), Richardson and Briggs[21] (crossed circles), and Richardson and Briggs[22] (crosses). The limiting values of porosity, $N_{\max}$ and $N_{\min}$, are discussed in the text. The theoretical curves labeled (a) $D = 3$ μm and (b) $D = 7$ μm and $D = 0.2$ μm represent Eq. (2.3), as evaluated using the cited values of the r.m.s. grain roughness. The key to the grain-size categories is: cs = coarse sand, ms = medium sand, fs = fine sand, and vfs = very fine sand.

has been plotted in Fig. 1(a), for comparison with the experimental data, under the simple assumption that the r.m.s. roughness is independent of the grain size with a value $D = 3$ μm. It is evident that the curve passes more or less through the middle of the data over a wide range (almost three decades) of grain size.

The expression for the porosity in Eq. (2.3) decreases monotonically with increasing grain size, asymptoting to $N_{\max} = 0.92$ and $N_{\min} = 0.37$ in the limits of small and large grain size, respectively. Physically, $N_{\min}$ represents a very coarse-grained material, where the roughness is negligible compared with the grain diameter and hence the grains pack together randomly in much the same way as smooth spheres. At the other limit, $N_{\max}$ is the porosity of a very fine-grained material in which the grain diameter is negligible in relation to the surface roughness.

Although the theoretical curve in Eq. (2.3) follows the trend of the porosity versus grain-size data in Fig. 1(a), it should be appreciated that the value of the grain roughness D for a particular sediment may differ from the nominal value $D = 3$ μm used in plotting the curve in Fig. 1(a). The point is illustrated in Fig. 1(b), where an additional data set from Richardson and Briggs[22] has been added to the data from Fig. 1(a). There is clearly a greater spread in the additional data, which is encompassed by the upper and lower theoretical curves in Fig. 1(b), as evaluated from Eq. (2.3) with $D = 7$ μm and $D = 0.2$ μm, respectively.

Porosity and grain size, both of which are often reported in sediment studies, together provide a means of inferring the value of D from Eq. (2.3). Direct measurements of the grain roughness, D, are not usually available, but clearly such measures would be useful in providing a test of the rough-surface model represented by Eq. (2.3). In the absence of a directly measured value for D, an estimate of the porosity from the grain size could be obtained from Eq. (2.3) using as a default value $D = 3$ μm. However, although usually yielding a porosity that is within a few percent of the actual value (see Fig. 1), this procedure should be treated with caution if the estimated value of N is to be used for deriving the wave properties of the sediment with high precision. As discussed below, the wave properties are very sensitive to the porosity, and it is recommended that, if possible, measured values of both the grain size and the porosity be used in evaluating the wave parameters.

In passing, it should be noted that immediately beneath the seawater-sediment interface the porosity is expected to be independent of depth in a homogeneous sediment. The reason for the depth-invariance is that the grains are in a close-packed (random) configuration. By definition, the packing cannot become any tighter with increasing depth: random close-packing holds all the way down, and thus the porosity remains constant (assuming the overburden pressure is not so great as to crush the grains). It follows from Eqs. (2.1) and (2.2) that the density and the bulk modulus are also expected to be independent of depth in the sediment.

Experimental evidence from core measurements supports the conclusion that the porosity is independent of depth immediately beneath the seawater-sediment interface. Richardson,[23] in his Fig. 2(b), shows the porosity profile of a fine sand from the continental shelf off Washington State, as measured from cores. The porosity was found to be essentially constant ($N \approx 0.4$) over depths down to 0.12 m where the sediment was homogeneous.

Below 0.12 m the sediment contained higher percentages of silt-sized particles, which gave rise to slightly increased values of the porosity. Cores from the West Florida Sand Sheet[21] also showed an essentially uniform porosity profile ($N \approx 0.4$) down to a depth of 0.2 m in the sediment. Similarly, in the recent SAX'99 experiment conducted in the northeastern Gulf of Mexico, preliminary results[24] from cores and from *in situ* electrical conductivity measurements indicate that the porosity is constant ($N \approx 0.38$) to a depth greater than 0.1 m in the medium sand sediment.

3. Waves in Unconsolidated Granular Materials

The theory of wave propagation in unconsolidated sediments, as developed by Buckingham,[17,18] is based on the idea that, in response to the dynamic strain associated with a wave propagating through the material, internal stress relaxation occurs via the mechanism of microscopic grain-to-grain shearing. In fact, two types of shearing are possible. The first is translational shearing in which the centers of two contiguous grains move relative to each other in a direction parallel to the tangent plane of contact; and the second is radial shearing, which occurs when the two contiguous grains are under dynamic compression or tension (i.e., negative compression). Radial shearing is perhaps less obvious than translational shearing and thus deserves a little explanation.

When two elastic spheres (i.e., mineral grains) are pressed together, for instance by the static overburden pressure, a flat circle of contact forms between them. Under an additional dynamic compression, as imposed by the passage of a wave, a further deformation of the two spheres occurs, which must result in sliding along the radials of the circle of contact. This sliding has to occur, even in the case of two spheres of equal size, because the circular surfaces of contact are not perfectly smooth but are covered with micro-asperities. Thus, contact between the spheres actually occurs at discrete points within the "circle of contact", where micro-asperities happen to form high spots. When the spheres deform as a wave passes, the micro-asperities in contact necessarily slide against one another, and, on average the shearing occurs axially symmetrically along the radials of the surface of contact.

The detailed behavior of the two shearing processes has been treated by Buckingham[18] in terms of a random stick-slip mechanism. This gives rise to a relationship between the internal stress and the rate of strain in the form of a convolution, actually two convolutions, one for translational and the other for radial shearing. The convolutions appear in the Navier–Stokes equation for the medium, which separates in a standard way into two wave equations, one for compressional and the second for shear disturbances.

The fact that a propagating shear wave emerges from the analysis may be surprising at first sight, in view of the fact that no intrinsic elasticity is included in the model. That is to say, the unconsolidated granular medium is taken to have no skeletal elastic frame. Indeed, this could be regarded as a defining property of an unconsolidated granular material, since the grains are not bonded together. The absence of an elastic frame is consistent with the observation that sands and other unconsolidated granular media do not behave symmetrically under compression and tension, and hence do not satisfy Hooke's

law: such materials support compression but under tension the unbonded grains simply separate.

According to the theory, the reason that a shear wave can propagate is that translational shearing between grains introduces shear rigidity into the medium; and rigidity in shear is exactly what is needed to support a transverse wave. Similarly, radial shearing gives rise to a bulk or "compressional" rigidity, which has no effect on the shear wave but raises the speed of the compressional wave slightly above the value, c_o, that it would have in the absence of grain-to-grain interactions, that is, if the medium were a simple two-phase mixture. Incidentally, it may help to think of the translational and radial shearing as being analogous to the shearing processes underlying the shear and bulk viscosity of a Newtonian fluid, although the analogy should not be pressed too far.

In addition to rigidity, both types of shearing introduce dissipation into the medium. According to the theory, the dissipation manifests itself, in both the compressional and the shear wave, as an attenuation that varies essentially as the first power of frequency. Now, the attenuation α, of a wave may be expressed in terms of the Q, or quality factor, through the defining expression

$$\alpha = \frac{|\omega|}{c}\frac{1}{2Q}\,, \tag{3.1}$$

where ω is angular frequency and c is the phase speed. In the geophysics literature, a wave whose attenuation scales linearly with the frequency is often described as having a constant Q, or sometimes a nearly-constant Q, the latter corresponding to the situation where the attenuation scales as f^s, where s is very close to unity. Considerable experimental evidence has accumulated to support the view that the attenuation of compressional[10,11] and shear[13,14] waves in granular materials, including unconsolidated marine sediments, exhibit a nearly-constant Q over many decades of frequency.

The frequency dispersion associated with a wave showing a nearly-constant Q has been discussed from a theoretical point of view by several authors, including Futterman,[25] Kjartansson,[26] and Horton.[27,28] All concluded that the dispersion is weak and approximately logarithmic in frequency. An identical result emerges from Buckingham's grain-to-grain shearing theory.[18,19] For the compressional wave, the theory predicts dispersion in the region of 1.5% per decade of frequency, which is consistent with laboratory measurements made in medium sand by Wingham,[29] and also with the preliminary results from the measurements performed by several groups during the SAX'99 experiments in the Gulf of Mexico.[24]

4. Attenuation-Dispersion Pairs

The expressions for the wave speeds and attenuations presented below are from Buckingham's theory of wave propagation in unconsolidated granular media.[17–19] These expressions depend on frequency, the physical properties of the material (density, porosity and grain size), and depth in the sediment. As discussed below, they also involve three unknown constants (γ_{op}, γ_{os}, and n), which characterize the shearing between grains and whose values

must be determined by comparison with data. In fact, the three items of data that are required to determine the constants are the shear wave speed and the shear wave attenuation (both at a specified frequency) and the compressional wave speed (also at a specified frequency, which may differ from that for the shear wave). The fourth wave property, which is not used in evaluating the constants, is the compressional wave attenuation. It follows that, as a test of the theory, the predicted compressional wave attenuation may be compared with experimental data. Such a test is performed below in Sec. 6.

According to the theory, the phase speed, c_p, and attenuation, α_p, of the compressional wave are given, respectively, by the expressions

$$\frac{1}{c_p} = \frac{1}{c_o}\mathrm{Re}\left[1 + \frac{\mu_p}{\rho_o c_o^2}(j\omega t_p)^n + \frac{4\mu_s}{3\rho_o c_o^2}(j\omega t_s)^m\right]^{-1/2} \tag{4.1}$$

and

$$\alpha_p = -\frac{\omega}{c_o}\mathrm{Im}\left[1 + \frac{\mu_p}{\rho_o c_o^2}(j\omega t_p)^n + \frac{4\mu_s}{3\rho_o c_o^2}(j\omega t_s)^m\right]^{-1/2} . \tag{4.2}$$

Similarly for the shear wave, the phase speed, c_s, and attenuation, α_s, are given by

$$\frac{1}{c_s} = \frac{1}{c_o}\mathrm{Re}\left[\frac{\mu_s}{\rho_o c_o^2}(j\omega t_s)^m\right]^{-1/2} \tag{4.3}$$

and

$$\alpha_s = -\frac{\omega}{c_o}\mathrm{Im}\left[\frac{\mu_s}{\rho_o c_o^2}(j\omega t_s)^m\right]^{-1/2} . \tag{4.4}$$

In these expressions, ω is angular frequency and c_o is the phase speed that the compressional wave would have if the granular material were a simple two-phase mixture with no grain-to-grain interactions, that is, if the medium were a suspension. The sound speed in this "equivalent suspension" is given by Wood's equation[30]:

$$c_o = \sqrt{\frac{\kappa}{\rho_o}}\,, \tag{4.5}$$

where ρ_o and κ are the density and bulk modulus of the granular material, as expressed in Eqs. (2.1) and (2.2).

Figure 2 shows c_o as a function of the porosity, N, as evaluated from Eqs. (2.1), (2.2), and (4.5). Note the broad minimum at $N = 0.78$, corresponding to a value of $c_o = c_{o\,\mathrm{min}} = 1431.4$ m/s, which is significantly less than the speed of sound in either the quartz (3560.8 m/s) or the seawater (1482.3 m/s) constituting the granular medium. As may be appreciated from Eq. (4.1), the presence of this minimum in c_o may explain why very fine-grained marine sediments (silts and clays), in which the porosity is close to 0.78 (see Fig. 1), show a compressional wave speed which is noticeably less than the speed of sound in the interstitial seawater.

The remaining parameters in Eqs. (4.1)–(4.4) are (μ_p, t_p, n) and (μ_s, t_s, m), where the two groups are representative, respectively, of radial shearing (under compression) and

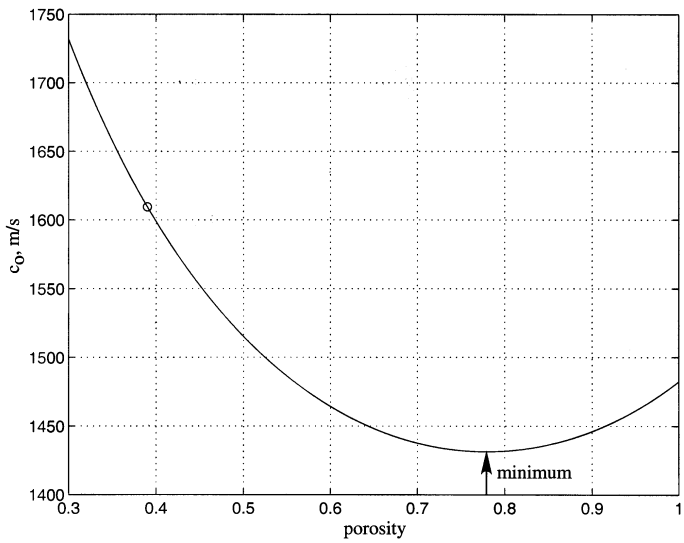

Fig. 2. Comprssional wave speed, c_o, in the equivalent suspension as a function of porosity (from Wood's equation, Eq. (4.5)). The circle represents the computed value of c_o for the SAX'99 sediment and the arrow identifies the minimum sound speed of 1431.4 m/s at a porosity of 0.78.

translational shearing. In both cases, the stress relaxation moduli, $\mu_{p,s}$, characterize the magnitude of the stress associated with shearing; the time constants $t_{p,s}$ are measures of the delay (which in practical terms is negligible) between the application of a dynamic strain and the ramping up of the induced stress as a micro-asperity at a contact between grains deforms elastically; and n, m are dimensionless exponents characterizing the very localized conservative and dissipative stresses associated with the sliding of individual micro-asperities at the contacts between grains.

The expressions in Eqs. (4.1) and (4.4) are examples of attenuation-dispersion pairs. These particular pairs satisfy causality, implying that they also satisfy the Kramers–Kronig relationships; and they are valid, in the sense of representing the translational and radial grain-shearing mechanisms, over the full frequency range from zero to infinity (or strictly from negative to positive infinity). Notice that, by including c_o explicitly, the expressions for the shear wave in Eqs. (4.3) and (4.4) have been written in such a way as to preserve a certain symmetry with those for the compressional wave in Eqs. (4.1) and (4.2). It should be clear, however, that c_o cancels out of Eqs. (4.3) and (4.4), and hence that the predicted properties of the shear wave are independent of c_o, as would be expected from physical considerations.

The time constants $t_{p,s}$ and the exponents n, m characterize, between them, the microscopic grain-shearing process, constituting the internal stress relaxation, that occurs in response to the application of a dynamic strain (i.e., a nonzero rate of strain). The stress relaxation occurs through the deformation of micro-asperities as they slide against one another on the surfaces of contact between contiguous grains. Since the deformation of micro-asperities is identical under translational and radial shearing, it follows that there

must be equality between the two time constants and also between the two stress relaxation exponents, that is,

$$t_p = t_s \tag{4.6}$$

and

$$n = m\,. \tag{4.7}$$

The latter equality, between n and m, is particularly important because it imposes a severe constraint on the predictions of the model. As discussed below, Eq. (4.7) implies that the wave properties (speeds and attenuations) of the compressional and the shear wave are not independent but are tightly coupled together.

The radial and translational stress relaxation moduli, μ_p and μ_s, depend on grain size, u_g, and depth, d, in the sediment, the latter dependence being due to the overburden pressure. The dependencies, however, are different for the two moduli: each is proportional to the number of micro-asperities involved in the sliding process, and this number scales as either the radius (for μ_p) or the area (for μ_s) of the circle of contact. From the Hertz theory of elastic spheres pressed together in contact,[31] it follows that

$$\mu_p = \mu_{op}\left(\frac{u_g d}{u_o d_o}\right)^{1/3}\,, \tag{4.8}$$

and

$$\mu_s = \mu_{os}\left(\frac{u_g d}{u_o d_o}\right)^{2/3}\,, \tag{4.9}$$

where μ_{op}, μ_{os} are constants, $u_o = 1000$ μm is a reference grain diameter (taken to be the same as that used in the ϕ units of grain size), and $d_o = 0.3$ m is a reference depth in the sediment, chosen because many measurements have been reported at a depth of 0.3 m by Hamilton, Richardson, and others. Comparison of Eqs. (4.1) and (4.3) with experimental data on the compressional and shear wave speeds indicates that the compressional stress relaxation constant, μ_{op}, is very much greater (by over an order of magnitude) than the shear stress relaxation constant, μ_{os}. As a consequence, as can be seen from Eqs. (4.1) and (4.2), the stiffness and dissipation associated with translational shearing have a negligible (but nonzero) effect on the compressional wave speed and attenuation.

When Eqs. (4.8) and (4.9) are substituted into Eqs. (4.1)–(4.4), the attenuation-dispersion pairs can be written as follows:

$$\frac{1}{c_p} = \frac{1}{c_o}\mathrm{Re}\left[1 + \frac{(3\gamma_p + 4\gamma_s)}{3\rho_o c_o^2}(j\omega T)^n\right]^{-1/2}\,, \tag{4.10}$$

$$\alpha_p = -\frac{\omega}{c_o}\mathrm{Im}\left[1 + \frac{(3\gamma_p + 4\gamma_s)}{3\rho_o c_o^2}(j\omega T)^n\right]^{-1/2}\,, \tag{4.11}$$

and

$$\frac{1}{c_s} = \frac{1}{c_o}\mathrm{Re}\left[\frac{\gamma_s}{\rho_o c_o^2}(j\omega T)^n\right]^{-1/2} = \sqrt{\frac{\rho_o}{\gamma_s}}|\omega T|^{-n/2}\cos\frac{n\pi}{4}\,, \tag{4.12}$$

$$\alpha_s = -\frac{\omega}{c_o}\mathrm{Im}\left[\frac{\gamma_s}{\rho_o c_o^2}(j\omega T)^n\right]^{-1/2} = |\omega|\sqrt{\frac{\rho_o}{\gamma_s}}|\omega T|^{-n/2}\sin\frac{n\pi}{4}\,, \tag{4.13}$$

where T is an entirely arbitrary reference time. The only reason for introducing T is to keep terms raised to the (fractional) power of n dimensionless; the presence of T does not reduce the generality of Eqs. (4.10)–(4.13), nor does the value of T have any effect on the wave speeds and attenuations predicted by these expressions. This last point should be obvious from the definitions of the new coefficients γ_p, γ_s, in which the stress relaxation moduli, μ_p, μ_s are amalgamated with the time constant $t_p = t_s$:

$$\gamma_p = \mu_p\left(\frac{t_p}{T}\right)^n = \gamma_{op}\left(\frac{u_g d}{u_o d_o}\right)^{1/3}, \quad \text{where} \quad \gamma_{op} = \mu_{op}\left(\frac{t_p}{T}\right)^n \tag{4.14}$$

and

$$\gamma_s = \mu_s\left(\frac{t_p}{T}\right)^n = \gamma_{os}\left(\frac{u_g d}{u_o d_o}\right)^{2/3}, \quad \text{where} \quad \gamma_{os} = \mu_{os}\left(\frac{t_p}{T}\right)^n. \tag{4.15}$$

From the formulation of Eqs. (4.10)–(4.15), it is evident that the wave speeds and attenuations depend on only three unknown constants, γ_{op}, γ_{os}, and n. These must be determined from a comparison with experimental data. It can be seen immediately, however, from inspection of Eq. (4.13) that the stress relaxation exponent, n, must be a very small number, that is $0 < n \ll 1$, since this is the condition that yields a shear wave with an attenuation varying essentially as the first power of frequency (i.e., a nearly-constant Q).

The attenuation-dispersion pairs in Eqs. (4.10)–(4.13) are exact and perfectly well behaved throughout the entire frequency range. The form of the frequency dependence is not, however, immediately apparent from these general expressions; trends in frequency are more easily appreciated by expanding Eqs. (4.10)–(4.13) in Taylor series in the small parameter, n. Bearing in mind that $\gamma_p \gg \gamma_s$, the following results hold to first-order in n:

$$c_p \approx c_o\sqrt{1+\Gamma_p}\left\{1 + \frac{1}{\pi Q_p}\ln|\omega T|\right\} \tag{4.16}$$

$$\alpha_p \approx \frac{|\omega|}{c_o\sqrt{1+\Gamma_p}}\frac{1}{2Q_p}\,, \tag{4.17}$$

where Q_p, the quality factor of the compressional wave, is given by

$$\frac{1}{Q_p} \approx \frac{n\pi\Gamma_p}{2(1+\Gamma_p)}\,; \tag{4.18}$$

and

$$c_s \approx c_o\sqrt{\Gamma_s}\left\{1 + \frac{1}{\pi Q_s}\ln|\omega T|\right\} \tag{4.19}$$

$$\alpha_s \approx \frac{|\omega|}{c_o\sqrt{\Gamma_s}}\frac{1}{2Q_s}\,, \tag{4.20}$$

where Q_s, the quality factor of the shear wave, is given by

$$\frac{1}{Q_s} \approx \frac{n\pi}{2}\,. \tag{4.21}$$

For brevity, the normalized, dimensionless quantities

$$\Gamma_{p,s} = \frac{\gamma_{p,s}}{\rho_o c_o^2} \tag{4.22}$$

have been used in these expressions.

A number of interesting conclusions, all valid to first-order in n, may be drawn from the approximations in Eqs. (4.16)–(4.21).

(1) The attenuation of both the compressional and the shear wave scales as the first power of frequency (i.e., in both cases the Q is independent of frequency).
(2) The Q-factor of the compressional wave is greater than that of the shear wave ($Q_p > Q_s$), by the factor $(1 + \Gamma_p)/\Gamma_p$.
(3) At any given frequency, the attenuation of the shear wave is very much greater than that of the compressional wave ($\alpha_s \gg \alpha_p$), by the factor $(c_p Q_p)/(c_s Q_s)$.
(4) Both the compressional and shear wave exhibit logarithmic dispersion at a level that scales inversely with the Q.
(5) Thus, the dispersion in the shear wave is greater than that in the compressional wave by the factor Q_p/Q_s.

The logarithmic approximations for the dispersion in Eqs. (4.16) and (4.19) have exactly the same form as that discussed by Futterman[25] and Kjartansson[26] for a wave with a constant Q. It should be noted that these logarithmic approximations are not well behaved at all frequencies, but diverge to negative infinity in the low frequency limit. In contrast, the exact forms in Eqs. (4.10) and (4.12) do not diverge but reduce, respectively, to $c_p = c_o$ and $c_s = 0$ at zero frequency, implying that in the low frequency limit grain-to-grain interactions have no effect on wave propagation in the sediment, which acts as a simple, lossless suspension. This should not be surprising in view of the fact that the internal stress arising from inter-granular shearing depends on the rate of strain, rather than the strain itself, and the rate of strain obviously vanishes at zero frequency.

This said, the logarithmic forms in Eqs. (4.16) and (4.19) are actually very good approximations over several decades of frequency around the point where $|\omega T| = 1$. It is interesting to note that, although the value chosen for T has no effect whatsoever on the exact expressions for the wave speeds and attenuations, it does control the accuracy of the approximations. The reason for this is that, when $|\omega T|^n$ is expanded in a Taylor series, the expansion parameter is actually not n but $(n \ln |\omega T|)$, which is identically zero when $|\omega T| = 1$. Thus, when $|\omega T| = 1$, the first term of the series is exact and the approximations represent most accurately the exact expressions for the sound speeds and attenuations.

It follows that, to match the approximations to broadband data, T should be selected such that $|\hat{\omega} T| = 1$, where $\hat{\omega}$ is the geometric mean of the upper and lower frequency limits between which the data were taken. Since compressional and shear wave data are usually

taken over distinctly different frequency ranges, the optimal value of T may be quite different for the two types of wave. Of course, the whole issue of selecting an appropriate value of T may be avoided by setting $T = 1\,\mathrm{s}$ and working with the exact expressions for the wave speeds and attenuations in Eqs. (4.10)–(4.13).

The approximations for the wave speeds in Eqs. (4.16) and (4.19) may be further simplified by neglecting the dispersion entirely, which is equivalent to neglecting all but the zero-order term in the Taylor series expansions. Thus, to the lowest (nonzero) order in n, the sound speed and attenuation, respectively, of the compressional wave are as follows:

$$c_p \approx c_o \sqrt{1 + \Gamma_p}\,, \tag{4.23}$$

$$\alpha_p \approx \frac{|\omega|}{4c_o} \frac{n\pi\Gamma_p}{(1+\Gamma_p)^{3/2}}\,, \tag{4.24}$$

and for the shear wave:

$$c_s \approx c_o \sqrt{\Gamma_s}\,, \tag{4.25}$$

$$\alpha_s \approx \frac{|\omega|}{c_o\sqrt{\Gamma_s}} \frac{n\pi}{4}\,. \tag{4.26}$$

(Obviously, the attenuations here are the same as in Eqs. (4.17) and (4.20)).

The approximate forms in Eqs. (4.23)–(4.26) have been compared with extensive data sets[17,18] of wave properties versus physical properties of marine sediments. The expressions yield a set of relationships, for instance compressional speed versus porosity, all of which follow the trends of the data very satisfactorily. In fact, the expressions in Eqs. (4.23)–(4.26) were used to generate representative marine sediment parameters for several of the test cases included in O.N.R.s recent SWAM'99 benchmark exercise. The accuracy of the approximations in Eqs. (4.16)–(4.21) and (4.23)–(4.26) is discussed below in Sec. 8, where they are compared with the exact forms in Eqs. (4.10)–(4.13).

Our present purpose is, not to fit the approximate theoretical expressions to trends in the data, but to be more precise by using the exact expressions in Eqs. (4.10)–(4.13), in conjunction with an accurately known value of the porosity, to predict one of the four wave properties of a specific marine sediment. The remaining three wave properties are used to determine the three unknown constants, n, γ_{op}, and γ_{os}, that appear in the theory.

5. Evaluation of the Three Unknown Constants, n, γ_{op}, and γ_{os}

The four exact expressions for the wave speeds and attenuations in Eqs. (4.10)–(4.13) involve just three unknown constants, n, γ_{op} and γ_{os}. These may be evaluated from measurements of the shear wave speed and the shear wave attenuation at a specified frequency, f_s, and the compressional wave speed at a frequency f_p. Note that the attenuation of the compressional wave is not required to determine the three constants, which is important because the comparison between the predicted and measured compressional attenuation then acts as a stringent test of the theory leading to Eqs. (4.10)–(4.13).

To determine n, it is necessary only to form the product of the shear wave speed and attenuation from Eqs. (4.12) and (4.13):

$$c_s \alpha_s = |\omega_s| \tan \frac{n\pi}{4} , \tag{5.1}$$

where $\omega_s = 2\pi f_s$. It follows from Eq. (5.1) that

$$n = \frac{4}{\pi} \tan^{-1} \left\{ \frac{c_s \alpha_s}{|\omega_s|} \right\} . \tag{5.2}$$

Note that α_s in Eq. (5.2) must be expressed in nepers/m, which is obtained by dividing dB/m by $20 \log_{10}(e) = 8.686$. Since α_s, c_s, and ω_s are all assumed to be known data, Eq. (5.2) specifies n uniquely.

To determine γ_{os}, the expression in Eq. (4.12) for the speed of the shear wave may be inverted to yield

$$\gamma_{os} = \frac{\rho_o c_s^2 \cos^2 \frac{n\pi}{4}}{|\omega_s|^n} \left(\frac{u_g d}{u_o d_o} \right)^{-2/3} , \tag{5.3}$$

where T has been set to the default value of $T = 1$ s. Usually, the grain size, u_g, is reported as part of the environmental data characterizing a sediment. If the porosity of the sediment is also available from a measurement, then the bulk density, ρ_o, appearing in Eq. (5.3) may be evaluated directly from Eq. (2.1). Alternatively, it would appear that the porosity could be evaluated from Eq. (2.3) using the nominal r.m.s. grain roughness of $D = 3$ μm, but this procedure may lead to an estimated porosity which differs slightly from the actual porosity. For estimating trends in the relationships between parameters, as was done previously,[17,18] such a small error is immaterial; but this is not so for the precision prediction under discussion. The predicted wave properties are very sensitive to the porosity, and thus a directly measured, accurate value of the porosity should be used in the computation.

Provided that the depth, d, of the shear wave measurement is known, Eq. (5.3) specifies γ_{os} uniquely. With n and γ_{os} determined, it is a straightforward matter to compute the remaining constant, γ_{op}, from Eq. (4.10) for the speed of the compressional wave. The speed c_o in this expression, and in Eq. (5.3), must of course be evaluated from Eq. (4.5) using an available value of the porosity.

Once all three constants, n, γ_{op}, and γ_{os}, have been evaluated for a particular sediment, the expressions in Eqs. (4.10)–(4.13) fully specify the wave properties of that medium. That is to say, these expressions provide the variation of the wave speeds and attenuations with frequency and with depth beneath the seawater-sediment interface. If it were found that the values of n, γ_{op}, and γ_{os} are invariant for all unconsolidated sandy sediments, then Eqs. (4.10)–(4.13) should also yield the wave properties as a function of grain size and of porosity. (As discussed earlier, although it is known that grain size and porosity are loosely correlated, small variations in grain roughness make it preferable to use independent measures of u_g and N if precise prediction of wave properties is an important objective.) It is possible, however, that n, γ_{op}, and γ_{os} may not be invariant for all sandy sediments

but may show a (weak) dependence on the r.m.s. grain roughness, D. If such were the case, then n, γ_{op}, and γ_{os} would have to be evaluated for each sediment as functions of D, using the procedure described above, in order to achieve a precise description of all the wave properties.

6. A Test of the Theory

For the purpose of evaluating the unknown constants and hence the wave properties, very few experimental data sets are available which adequately characterize a sandy sediment. The required data are: grain size, u_g; porosity, N; shear wave speed, c_s; shear wave attenuation, α_s; compressional wave speed, c_p; and compressional wave attenuation, α_p. One medium-sand site for which all these data have been determined is in the northeastern Gulf of Mexico off the Florida Panhandle, where the SAX'99 multi-institutional experiment was conducted in September–November 1999 as part of an O.N.R. research initiative on high-frequency sound interaction in ocean sediments.

Preliminary data for the SAX'99 site, as reported by Richardson *et al.*,[24] are presented in Table 1. Note that to match Eq. (2.3) precisely to the measured grain size ($u_g = 379$ μm) and porosity ($N = 0.39$), the grain roughness must be set to $D = 2.08$ μm, indicating that at this site the grains are a little smoother than those of the "default sediment". With D set to the default value of 3 μm, the predicted porosity is $N = 0.3986$, which, although only 2% higher than the measured value, is nevertheless sufficient to change the predicted compressional attenuation by about 1 dB/m at a frequency of 38 kHz.

By using the inversion technique outlined in Sec. 5, the three unknown constants in the theory are found to be: $n = 0.09014$, $\gamma_{op} = 3.710 \times 10^8$ Pa, and $\gamma_{os} = 2.898 \times 10^7$ Pa. Now, it will be recalled that the attenuation of the compressional wave is not involved in the evaluation of these constants. As a test of the theory, these values may therefore be

Table 1. Parameters for the SAX'99 site, as reported by Richardson *et al.*[24]

Sediment Property	SAX'99 Measured Values	Comments
grain size, u_g μm (ϕ)	379 (1.4)	from diver cores
porosity, N	0.39	from *in situ* electrical conductivity probe
shear dB/m atten., α_s (nepers/m)	30 (3.45)	from ISSAMS @ 1 kHz
shear speed, c_s, m/s	129	from ISSAMS @ 1 kHz, $d = 0.3$ m
comp. speed, c_p, m/s	1739	from ISSAMS @ 38 kHz
comp. dB/m atten., α_p (nepers/m)	12.7 (1.46)	from ISSAMS @ 38 kHz

substituted into Eq. (4.11), which yields $\alpha_p = 12.17$ dB/m at 38 kHz. This theoretical prediction may be compared with the observed value of 12.7 dB/m at 38 kHz. Thus, the predicted attenuation is just 0.53 dB/m lower than the (mean) measured attenuation of the compressional wave at the SAX'99 site.

It is interesting to perform the same calculation but using, instead of the measured porosity $N = 0.39$ in Table 1, the porosity $N = 0.3986$ computed from Eq. (2.3) with $u_g = 379$ μm and the grain roughness set to the default value $D = 3$ μm. Then the predicted attenuation of the compressional wave is $\alpha_p = 12.99$ dB/m at 38 kHz, which is 0.3 dB/m higher than the measured value shown in Table 1. This serves to emphasize the sensitivity of the wave properties to the value of the porosity that is input to the model. Of course, predicting the compressional attenuation to within 0.5 dB/m of the measured value represents a high degree of precision. Yet, for the SAX'99 site, this level of agreement, at least with the preliminary data, is achieved by the grain-shearing theory described above.

7. *Q*-Factors, Attenuation and Dispersion for the SAX'99 Site

For convenience, the values of all the derived theoretical parameters for the SAX'99 site are listed in Table 2. These parameters were determined from the geoacoustic properties of the site listed in Table 1 (but excluding the compressional wave attenuation). Note that the compressional wave speed in the equivalent suspension is $c_o = 1609.4$ m/s, as indicated by the small circle in Fig. 2; and that at any given frequency, say 1 kHz, the attenuation of the shear wave is greater than that of the compressional wave by a factor of approximately 90. As noted earlier, this high value comes about because $c_p Q_p \gg c_s Q_s$.

The Q of a wave is related to the attenuation, α, and phase speed, c, as shown in Eq. (3.1). For the SAX'99 site, using the wave speed and attenuation data cited in Table 1, this yields $Q_p = 47.02$ and $Q_s = 7.06$. From the logarithmic approximations for the wave speeds in Eqs. (4.16) and (4.19), it is evident that these values of Q give rise to dispersion

Table 2. Values of the theoretical parameters for the SAX'99 site.

Parameter	Comments
$n = 0.09014$	
$\gamma_{os} = 2.898 \times 10^7$ Pa	
$\gamma_{op} = 3.710 \times 10^8$ Pa	
$\rho_o = 2015.7$ kg/m^3	
$\kappa = 5.22 \times 10^9$ Pa	
$c_o = 1609.4$ m/s	
$Q_s = 7.06$	
$Q_p = 47.02$	
$D = 2.08$ μm	
$\alpha_p = 12.17$ dB/m	predicted @ 38 kHz

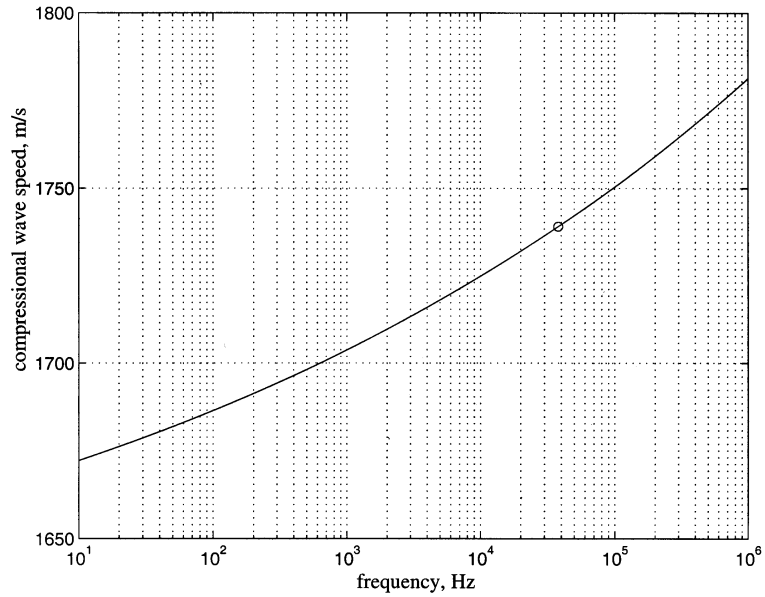

(a)

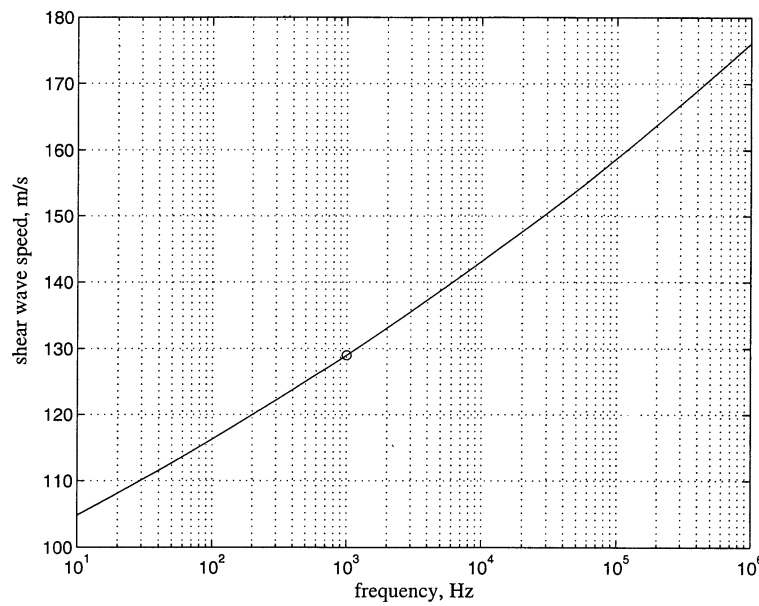

(b)

Fig. 3. Dispersion in (a) the compressional wave speed, c_p, and (b) the shear wave speed, c_s, as computed using the values of the theoretical constants appropriate to the SAX'99 sediment. The circles, representing the values of the wave speed, as measured using ISSAMS,[24] fall precisely on the theoretical curves because these data were used in determining the theoretical constants (see text).

in the compressional wave at a level of 1.6% per decade of frequency and in the shear wave of 10.4% percent per decade. The much higher level of dispersion in the shear wave could make it easier to detect experimentally than the comparatively weak dispersion in the compressional wave.

Figures 3(a) and (b) show the dispersion in the compressional and shear wave, as computed from the exact expressions for the wave speeds in Eqs. (4.10) and (4.12), respectively, using the values of the parameters in Table 2. The corresponding attenuations, from Eqs. (4.11) and (4.13), are shown as functions of frequency in Fig. 4. The small circles in Figs. 3 and 4 represent the data that were used in evaluating the parameters in the model; and the asterisk in Fig. 4 represents the measured value of the compressional wave attenuation, which was not used in the evaluation of the theoretical parameters. The datum represented by the asterisk is included in the figure to provide a visual comparison with the theoretically predicted curve for the attenuation of the compressional wave as a function of frequency.

It is evident from Fig. 4 that, according to the theory, the attenuation of the compressional and of the shear wave varies essentially as the first power of frequency, indicating a nearly constant Q in both cases. Such behavior is consistent with many observations of attenuation in saturated sediments that have been reported in the literature.[10–14] At present, the associated dispersion, particularly in the shear wave, is more difficult to verify because so

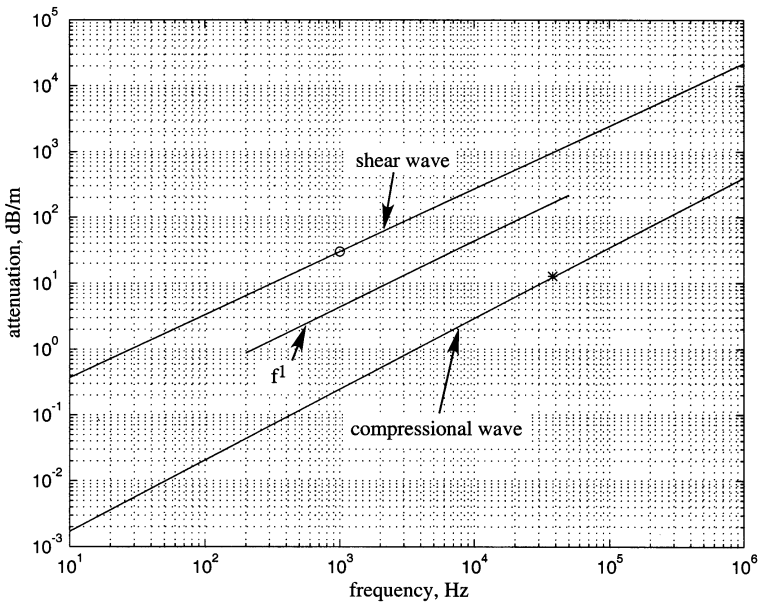

Fig. 4. Curves of attenuation versus frequency, as computed using the values of the three theoretical constants appropriate to the SAX'99 sediment. The circle and asterisk both represent data obtained using ISSAMS.[24] The circle falls precisely on the curve for attenuation in shear because this data point was used in determining the three constants. The asterisk lies approximately 0.5 dB/m above the predicted curve for the compressional attenuation (see text). The reference line labeled f^1 represents an attenuation that scales as the first power of frequency.

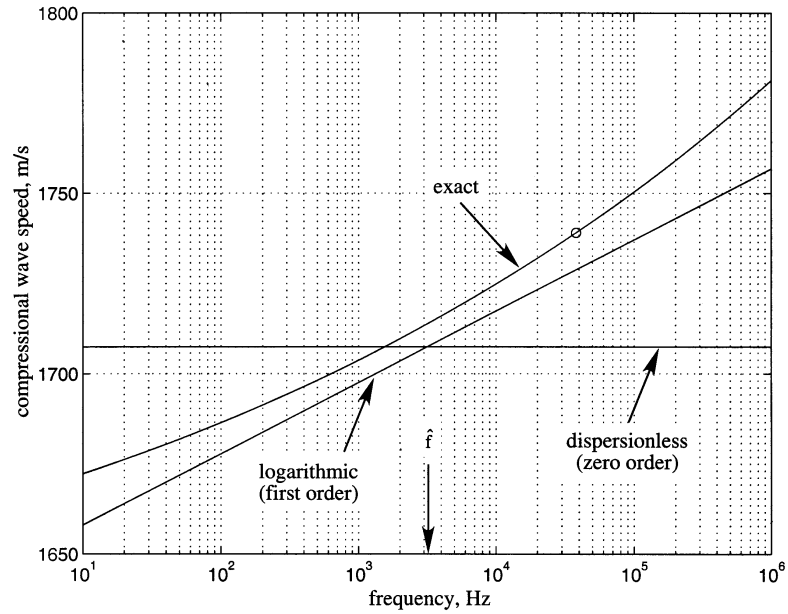

(a)

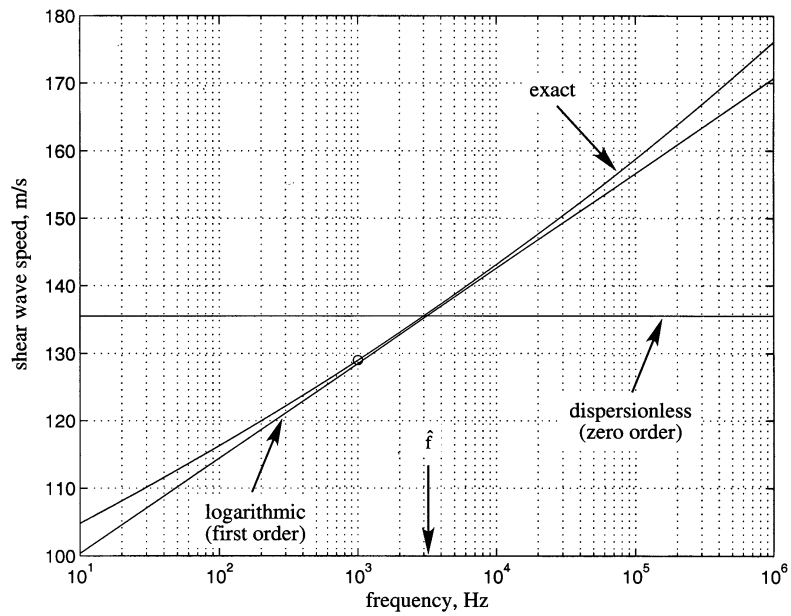

(b)

Fig. 5. Comparison between the exact nd approximate expressions for the wave speeds. The circles are the SAX'99 data points used in determining the unknown constants in the theory. (a) The compressional wave speed, showing Eqs. (4.10) (exact), (4.16) (logarithmic) and (4.23) (dispersionless). (b) The shear wave, showing Eqs. (4.12) (exact), (4.19) (logarithmic) and (4.25) (dispersionless).

few broadband measurements are available for comparison. It will be appreciated, however, that if a sediment (or any other linear medium) exhibits a nearly-constant Q, as exemplified in Fig. 4, then causality and the uniqueness of the Kramers–Kronig relationships dictate that the dispersion must be as shown in Figs. 3(a) and (b).

8. Accuracy of the Approximations

The approximate expressions for the wave speeds and attenuations in Eqs. (4.16)–(4.21) and (4.23)–(4.26) match the exact forms in Eqs. (4.10)–(4.13) reasonably well over many decades of frequency. This is illustrated for the SAX'99 parameters in Figs. 5 and 6, which show, respectively, comparative plots of the exact and approximate wave speeds and attenuations as functions of frequency. The exact curves in these figures are identical to those in Figs. 3 and 4. In evaluating the approximations, the value of T was taken to be $T = (2\pi\hat{f})^{-1}$, where $\hat{f} = 3.16$ kHz is the geometric mean of the upper and lower limits on the bandwidth shown in the figures. It should be borne in mind that, according to Eqs. (4.14) and (4.15), the values of γ_{op} and γ_{os} cited in Table 2 must be modified in the approximate expressions by the factor T^{-n}.

In Fig. 5(a), it is evident that the slope of the logarithmic approximation (Eq. (4.16)) is similar to that of the exact expression for the compressional wave speed. The magnitude of this approximation is slightly low, by about 0.6% (less than 10 m/s) at the origin of the Taylor expansion where $f = \hat{f}$, because Γ_s has been neglected in Eq. (4.16). It is, of

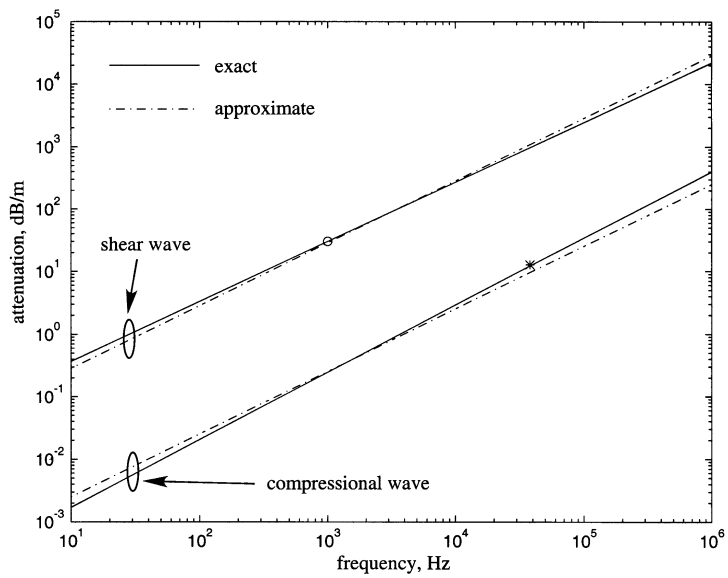

Fig. 6. Comparison between the exact and approximate expressions for the attenuations. The circle is the SAX'99 data point for the shear attenuation that was used in determining the unknown constants in the theory, and the asterisk is the measured compressional wave attenuation. For the compressional wave, the exact curve was computed from Eq. (4.11) and the first-order approximation from Eq. (4.24). For the shear wave, the exact and approximate curves were computed from Eqs. (4.13) and (4.26), respectively.

course, a trivial matter to include Γ_s in the approximations, in which case all three curves in Fig. 5(a) would be essentially coincident at $f = \hat{f}$.

The logarithmic approximation for the shear wave speed (Eq. (4.19)) provides an excellent match to the exact expression (Eq. (4.12)) over three or more decades of frequency, as can be seen in Fig. 5(b). In this case, the three curves essentially coincide at the origin of the Taylor expansion for $|\omega T|^n$, where $f = \hat{f}$. (The curves do not precisely coincide at the origin because of the truncated Taylor expansion for j^n.)

Figure 6 shows the comparison between the exact (Eqs. (4.11) and (4.13)) and the approximate (Eqs. (4.24) and (4.26)) expressions for the compressional and shear wave attenuations. Agreement between the exact and approximate forms is excellent over several decades of frequency. Note that the approximation slightly underestimates the slope in the case of the compressional wave and slightly overestimates it in the case of the shear wave. For most practical purposes, however, these small differences are of little consequence because they lie well within the accuracy of most measurements.

9. Concluding Remarks

The results of a theoretical model of wave propagation in unconsolidated granular media have been presented and discussed in this article. Four equations are given which specify the compressional and shear wave speeds and the associated attenuations. All four of these wave properties depend on frequency as well as on grain size and porosity. In fact, the wave properties are particularly sensitive to the porosity, which must be specified as precisely as possible if accurate predictions are to be obtained.

As a test of the theory, a preliminary data set from the SAX'99 experiment, which was performed recently in the Gulf of Mexico, is considered in the paper. Three items of the wave data (compressional speed, shear speed and shear attenuation) are used to determine the three unknown constants that appear in the theoretical expressions. The fourth wave parameter, the compressional attenuation, is then evaluated from the theory and shown to match the measured value to within 0.5 dB/m at a frequency of 38 kHz.

Although this high level of agreement between theory and experiment has been demonstrated for only a single site, the only one for which an adequate geoacoustic data set exists in the literature, it does indicate that the wave properties of sediments are not independent but are strongly correlated. That is to say, given three of the wave properties, the fourth can be accurately predicted (with the provision that the porosity is known with some precision). According to the theoretical model, the correlations exist because all four wave properties are causally connected: the central physical mechanism that governs these properties is the sliding of one micro-asperity against another on the surfaces of contact between contiguous grains.

Acknowledgment

This work was supported by the Office of Naval Research under Grant No. N00014-91-J-1118.

References

1. D. L. Johnson and T. J. Plona, "Acoustic slow waves and the consolidation transition," *J. Acoust. Soc. Am.* **72**, 556 (1982).
2. H. J. Simpson and B. H. Houston, "A synthetic array measurement of a fast compressional and a slower wave in an unconsolidated water-saturated porous medium," *J. Acoust. Soc. Am.* **102**, 3210 (1997).
3. H. J. Simpson and B. H. Houston, "Analysis of laboratory measurements of sound propagating into an unconsolidated water-saturated porous media," *J. Acoust. Soc. Am.* **103**, 3095 (1998).
4. H. J. Simpson, B. H. Houston, and L. S. Couchman, "Measurements and modeling of sound propagating into unconsolidated water-saturated porous media in a laboratory environment," *J. Acoust. Soc. Am.* **104**, 1787 (1998).
5. H. J. Simpson and B. H. Houston, "Synthetic array measurements of acoustical waves propagating into a water-saturated sandy bottom for a smoothed and a roughened interface," *J. Acoust. Soc. Am.* **107**, 2329 (2000).
6. M. A. Biot, "Theory of propagation of elastic waves in a fluid-saturated porous solid: I. Low-frequency range," *J. Acoust. Soc. Am.* **28**, 168 (1956).
7. M. A. Biot, "Theory of propagation of elastic waves in a fluid-saturated porous solid: II. Higher frequency range," *J. Acoust. Soc. Am.* **28**, 179 (1956).
8. T. J. Plona, "Observation of a second bulk compressional wave in a porous medium at ultrasonic frequencies," *Applied Physics Letters* **36**, 259 (1980).
9. M. R. Wyllie, A. R. Gregory, and L. W. Gardner, "Elastic wave velocities in heterogeneous and porous media," *Geophys.* **21**, 41 (1956).
10. E. L. Hamilton, "Compressional-wave attenuation in marine sediments," *Geophys.* **37**, 620 (1972).
11. E. L. Hamilton, "Acoustic properties of sediments," in *Acoustics and the Ocean Bottom*, eds. A. Lara-Saenz, C. R. Cuierra, and C. Carbo-Fité (Consejo Superior de Investigacions Cientificas, Madrid, 1987), pp. 3–58.
12. L. Bjørnø, "Features of the linear and non-linear acoustics of water-saturated marine sediments," Technical Report AFM76-06, Technical University of Denmark, June 1976.
13. B. A. Brunson and R. K. Johnson, "Laboratory measurements of shear wave attenuation in saturated sand," *J. Acoust. Soc. Am.* **68**, 1371 (1980).
14. B. A. Brunson, "Shear wave attenuation in unconsolidated laboratory sediments," in *Shear Waves in Marine Sediments*, eds. J. M. Hovem, M. D. Richardson, and R. D. Stoll (Kluwer, Dordrecht, 1991), pp. 141–147.
15. E. L. Hamilton and R. T. Bachman, "Sound velocity and related properties of marine sediments," *J. Acoust. Soc. Am.* **72**, 1891 (1982).
16. M. D. Richardson, "In-situ, shallow-water sediment geoacoustic properties," in *Shallow-Water Acoustics*, eds. R. Zhang and J. Zhou (China Ocean Press, Beijing, China, 1997), pp. 163–170.
17. M. J. Buckingham, "Theory of acoustic attenuation, dispersion, and pulse propagation in unconsolidated granular materials including marine sediments," *J. Acoust. Soc. Am.* **102**, 2579 (1997).
18. M. J. Buckingham, "Theory of compressional and shear waves in fluid-like marine sediments," *J. Acoust. Soc. Am.* **103**, 288 (1998).
19. M. J. Buckingham, "Wave propagation, stress relaxation, and grain-to-grain shearing in saturated, unconsolidated marine sediments," *J. Acoust. Soc. Am.* **108**, 2796 (2000).
20. E. L. Hamilton, "Sound velocity and related properties of marine sediments, North Pacific," *J. Geophys. Res.* **75**, 4423 (1970).
21. M. D. Richardson and K. B. Briggs, "In situ and laboratory geoacoustic measurements in soft

mud and hard-packed sand sediments: Implications for high-frequency acoustic propagation and scattering," *Geo-Marine Letters* **16**, 196 (1996).
22. M. D. Richardson and K. B. Briggs, "On the use of acoustic impedance values to determine sediment properties," in *Proceedings of the Institute of Acoustics*, vol. 15, eds. N. G. Pace and D. N. Langhorne (University of Bath, Bath, 1993), pp. 15–24.
23. M. D. Richardson, "Spatial variability of surficial shallow water sediment geoacoustic properties," in *Ocean-Seismo Acoustics: Low-Frequency Underwater Acoustics*, eds. T. Akal and J. M. Berkson (Plenum, New York, 1986), pp. 527–536.
24. M. D. Richardson, K. B. Briggs, D. L. Bibee, P. A. Jumars, W. B. Sawyer, D. B. Albert, T. B. Berger, M. J. Buckingham, N. P. Chotiros, P. H. Dahl, *et al.*, "Overview of SAX'99: Environmental considerations," *IEEE J. Ocean. Eng.* in review (2000).
25. W. I. Futterman, "Dispersive body waves," *J. Geophys. Res.* **67**, 5279 (1962).
26. E. Kjartansson, "Constant Q-wave propagation and attenuation," *J. Geophys. Res.* **84**, 4737 (1979).
27. C. W. Horton Sr., "Dispersion relationships in sediments and sea water," *J. Acoust. Soc. Am.* **55**, 547 (1974).
28. C. W. Horton Sr., "Comment on 'Kramers–Kronig relationship between ultrasonic attenuation and phase velocity' (*J. Acoust. Soc. Am.* **69** (1981), 696–701)," *J. Acoust. Soc. Am.* **70**, 1182 (1981).
29. D. J. Wingham, "The dispersion of sound in sediment," *J. Acoust. Soc. Am.* **78**, 1757 (1985).
30. A. B. Wood, *A Textbook of Sound*, 3rd edition (G. Bell and Sons Ltd., London, 1964).
31. S. P. Timoshenko and J. N. Goodier, *Theory of Elasticity*, 3rd edition (McGraw-Hill, New York, 1970).